# Ultrafast and Large Optical Nonlinearity of $TiSe_2$ Saturable Absorber in the 2 μm Wavelength Region

**Rongfei Wei,[1*] Xiangling Tian,[2,3*] Lupeng Yang,[1] Dandan Yang,[2] Zhijun Ma,[2] Hai Guo,[1] and Jianrong Qiu[2,4*]**

*[1]Department of Physics, Zhejiang Normal University, Jinhua, Zhejiang, 321004, China*

*[2]State Key Laboratory of Luminescent Materials and Devices, School of Materials Science and Engineering, South China University of Technology, Wushan Road 381,Guangzhou 510641, PR China*

*[3]Division of Physics and Applied Physics, School of Physical and Mathematical Sciences, Nanyang Technological University, 21 Nanyang Link, Singapore 637371, Singapore*

*[4]State Key Laboratory of Modern Optical Instrumentation, College of Materials Science and Engineering, Zhejiang University, Hangzhou, Zhejiang 310027, PR China.*

**rfwei@zjnu.edu.cn; xianglingt@sina.com; qjr@scut.edu.cn*

# Supporting Information

## 1. Experimental Section

**Materials preparation and characterization.**

Multilayer $TiSe_2$ were prepared by liquid phase exfoliation. In briefly, bulk 1*T*-$TiSe_2$ power (purchased from Aladdin Reagent Inc.) was treated by ultrasonic vibration in N-Methyl-2-pyrrolidone (NMP) for about 30 min.[1] The dispersion was centrifuged at 5000 rpm, and then $TiSe_2$ were obtained from the top of the transparent solution. In order to characterize $TiSe_2$, the sample was prepared by spin-coating the $TiSe_2$ solution onto a 0.5 mm thick high-purity fused silica at 500 rpm for 10 min.[2] After that, the sample was dried for 24 h in a vacuum oven. In order to accelerate the volatilization of NMP, appropriate amount of ethanol was added into the solution. The optical absorption spectra were recorded using a spectrophotometer (Elmer Lambda-900 UV/Vis/NIR, Waltham, MA) versus an uncoated quartz substrate as reference. Raman characterization was measured using a confocal microscopy system (RenishaiwnVia, Gloucestershire, UK) excited by a 532 nm laser. X-ray photoemission spectroscopy (XPS, K-Alpha, Thermo Science, UK) was employed to characterize the binding energies of the Se and Ti. X-ray diffraction (XRD) pattern was carried out by a Bruker diffractometer utilizing Cu K$\alpha$ radiation ($\lambda$=1.5418 Å). Atomic force microscopy (AFM, Nanoscope IIIa, Veeco) was used to record the thickness of $TiSe_2$.

## 2. Caculation of the nonlinear optical parameter.

Briefly, the nonlinear optical (NLO) theory was used to fit the open-aperture (OA) Z-scan datum by according the following formula:[3-6]

$$\frac{dI(z')}{dz'} = -\alpha_0 I(z') - \beta I^2(z') \qquad \text{(S1).}$$

Here $I(z')$ is the laser beam irradiance within the sample; $z'$ is the propagation distance in the sample; $\alpha_0$ and $\beta$ present the linear absorption coefficient of the sample and the nonlinear storable absorption coefficient, respectively. Hence, open-aperture Z-scan data can be fitted by the following equation:

$$T(z, S = 1) = \sum_{m=0}^{\infty} \frac{[-q_0(z)]^m}{(m+1)^{3/2}} \qquad \text{(S2).}$$

where $q_0(z)=\beta I_0 L_{eff}/(1+z^2/z_R^2)$, $I_0$ presents the on-axis intensity at the beam waist, $L_{eff}$ presents the effective length, and $z_R$ presents the Rayleigh length of the incident femtosecond laser beam. The

effective length can be described by the following relathionship:

$$L_{\text{eff}} = \int_0^L \exp(\alpha_0 z')dz' = \frac{1 - e^{-\alpha_0 L}}{\alpha_0} \quad \text{(S3)}$$

where, L is the thickness of the samples.

The imaginary part of the third-order nonlinear susceptibility can be obtained following:

$$\text{Im}\chi^{(3)}(\text{esu}) = \frac{10^{-7}\lambda c^2 n_0^2}{96\pi^2}\beta \quad \text{(S4).}$$

Here, $c$, $\lambda$, and $n$ are, respectively, the speed of light in the vacuum, the wavelength of incident light, and the refractive index.

Then, from the division of the closed-aperture Z-scan by the corresponding OA result, can be well fitted by the following formula:

$$T = 1 + \frac{4x\Delta\Phi}{(1+x^2)(9+x^2)} + \frac{4(3x^2-5)\Delta\Phi^2}{(1+x^2)^2(9+x^2)(25+x^2)} + \frac{32(3x^2-11)x\Delta\Phi^3}{(1+x^2)^3(9+x^2)(25+x^2)(49+x^2)} \quad \text{(S5).}$$

Here, the on-axis nonlinear phase shift at the focus is $\Delta\Phi = kI_0(n_2 L_{\text{eff}} + n_{2-\text{quartz}} L_{\text{quartz}})$, here, $n_2$ describes nonlinear refractive index of materials and $n_{2\text{-quartz}}$ describes nonlinear refractive index of fused quartz substrate, which is about $2.0\times10^{-7}$ cm$^2$ GW$^{-1}$; $L_{\text{quartz}}$ is the thick of fused silica; $k$ is the wavelength number; $x=z/z_R$ presents the dimensionless relative position from the waist; $n_2$ presents nonlinear refractive index. Therefore we obtained the real part of the third-order nonlinear susceptibility from the following relation:

$$\text{Re}\chi^{(3)}(\text{esu}) = \left[\frac{10^{-7} cn^2}{48\pi^2}\right] n_2 \quad \text{(S6).}$$

The figure of merit (FOM) is calculated as:

$$\text{FOM} = \left|\frac{\text{Im}\chi^{(3)}}{\alpha_0}\right|. \quad \text{(S7)}$$

**3. 2.0 μm fiber laser setup.**

The constructed Q-switched Tm-doped fiber (TDF) laser cavity are based on $TiSe_2$ saturable absorber. A commercial 793 nm laser diode (BWT, Beijing) with a multimode fiber pigtail (core diameter: 105

μm; circular core diameter: 10 μm; numerical aperture: 0.22) was used as the pump source to stimulate the gain fiber. A coupler (50:50, IFT, Canada) was employed to output half of the signal laser. In order to maintain the intra-cavity laser propagate unidirectionally, a PI-ISO was constructed in the laser cavity. The $TiSe_2$/poly(vinyl alcohol) (PVA) film was constructed between two FC/PC connectors as the saturable absorber. A PC was employed to control the intra-cavity loss. An InGaAs photodetector (EOT ET-5000F, USA) equipped with an 8 GHz digital oscilloscope was used to monitor the temporal pulse train and single pulse waveforms. The radio frequency (RF) spectrum was recorded by a RF spectrum analyzer (YIAI, China, AV4033A, 30Hz-18GHz). The optical spectrum was investigated using an optical spectrum analyzer (Yokogawa AQ6375, Japan) with a resolution of 0.05 nm. The output power was recorded using a thermal power sensor (S470C, Thorlabs, USA).

## 4. Results and Discussion.

Traditional optical pump-probe studies of TMDCs are generally focused on the investigation of resonant or near-resonant 1*s*-interband excitonic nonlinearities through adjusting the probe wavelength close to the exciton line.[7-9] Due to the band gap of TMDCs, both visible and near-infrared (NIR) pulses are usually employed as optical pump,[10-13] as schematically illustrated in Figure S1. In order to match the different response of photo-induced carriers, probe photon energies from the NIR to mid-infrared (MIR) region are typically utilized to investigate various kinds of bound and unbound carriers.[14-18] In contrast to NIR spectrum, MIR spectrum probe is sensitive to free carriers and weakly bound carriers due to the low probe energy.[7, 9, 15] In particular, if close to the excitonic resonances or intra-excitonic resonances, MIR spectrum probe is also utilized to investigate the strongly bound carriers. Further consideration of $TiSe_2$ with a very small gap (<150 meV), it is difficult to implement excitonic resonance probe measurements by a long-wavelength probe (>10 μm) due to technical restriction. Comparing all results obtained from pump-probe methods under the pump of visible or NIR, photo-induced carrier dynamics in TMDCs or $Cd_3As_2$ are clearly described,[19, 20] revealing thermal scatter effect (*e.g.*, electron-electron coupling and electron-phonon coupling) in detail. Therefore, NIR is utilized to be as pump-probe source to measure the changes in the $TiSe_2$, as depicted in Figure S1.

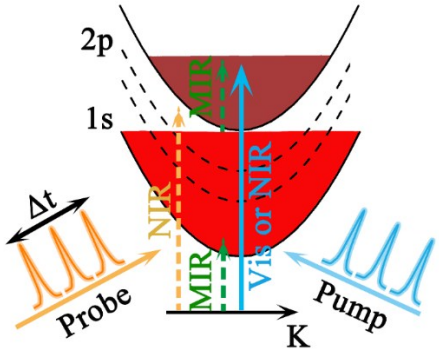


**Fig.S1.** Schematic diagram of multiple ultrafast pump-probe process. The relaxation pathways for the photo-induced carriers with optional excitation of visible (Vis), near-infrared (NIR) and mid-infrared (MIR). Solid line presents pump pulses and dashed line denotes possible transition by probe pulses.

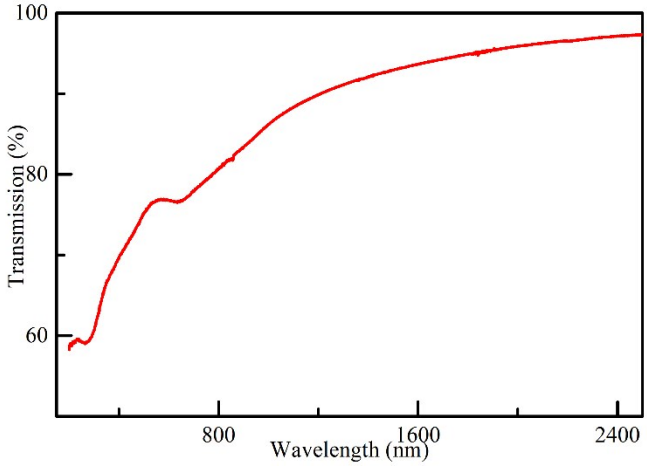


**Fig. S2.** The linear transmittance of $TiSe_2$.

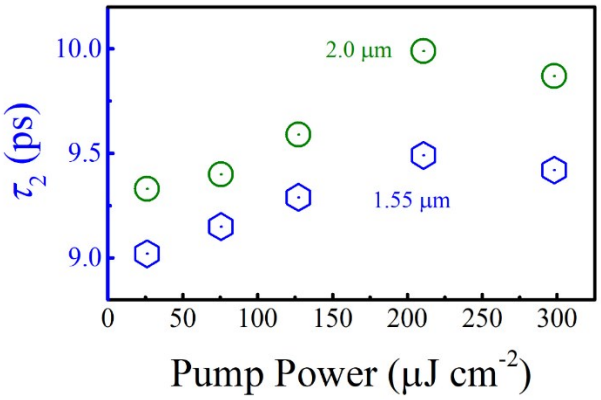


**Fig. S3.** The slow time component as a function of pump fluence.

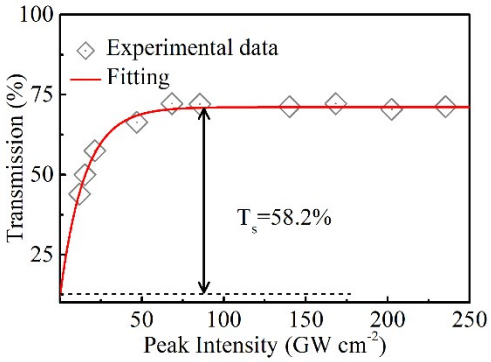


**Fig. S4.** Transmittance as a function of pulse peak intensity. The red line is fitting curve by by $T(I)=1-\Delta T\times\exp(-I/I_{sat})-T_{ns}$, in which , $I$, $T$, $I_{sat}$, and $T_{ns}$ are the input intensity, modulation depth, saturable intensity and nonsaturable absorbance, respectively.

**Table S1 NLO parameters of several typical materials**

| Laser | Sample | $\beta$ (cm GW$^{-1}$) | $n_2$ (cm$^2$ GW$^{-1}$) |
|---|---|---|---|
| 1030 nm, 1kHz, 340 fs | $MoS_2$ [21] | -(9.17±2.56)×10$^{-2}$ | N/A |
| | $MoSe_2$ [21] | -(1.29±0.13)×10$^{-2}$ | N/A |
| | $MoTe_2$ [21] | -(7.50±0.47)×10$^{-3}$ | N/A |
| | Graphene [21] | -(9.40±3.18)×10$^{-2}$ | N/A |
| 1550 nm, 35fs | Black Phosphorus [22] | -0.15×10$^{-3}$ | N/A |
| 1240 nm, 150 fs, 1kHz | ITO film [23] | -7000~-8000 | 0.11 |
| 1420 nm, | ITO fiml/Gold [24] | 2×10$^4$ | 3.73 |
| 1500 nm, 35 fs, 1kHz | ITO NCs [25] | -51.4 | N/A |
| 1300 nm | AZO films [26] | N/A | 0.17 |
| 1550 nm, 150 fs | SWNTs [27] | N/A | 10$^{-10}$ |
| 800 nm, 220 fs | Au nanorodes [28] | -1.5 | -1.2×10$^{-12}$ |
| 1550 nm 120 fs | $TiSe_2$ [a] | -0.17 | 0.088 |
| 2000 nm 120 fs | $TiSe_2$ [a] | -0.10 | 0.091 |

[a]This work


1. B. Yan, B. Zhang, H. Nie, G. Li, X. Sun, Y. Wang, J. Liu, B. Shi, S. Liu and J. He, *Nanoscale*, 2018, **10**, 20171-20177.
2. W. Wang, W. Yue, Z. Liu, T. Shi, J. Du, Y. Leng, R. Wei, Y. Ye, C. Liu, X. Liu and J. Qiu, *Adv. Opt. Mater.*, 2018, **6**, 1700948.
3. R. Wei, H. Zhang, X. Tian, T. Qiao, Z. Hu, Z. Chen, X. He, Y. Yu and J. Qiu, *Nanoscale*, 2016, **8**, 7704-7710.
4. X. Tian, R. Wei, M. Liu, C. Zhu, Z. Luo, F. Wang and J. Qiu, *Nanoscale*, 2018, **10**, 9608-9615.
5. R. Wei, H. Zhang, X. He, Z. Hu, X. Tian, Q. Xiao, Z. Chen and J. Qiu, *Opt. Mater. Express*,

2015, **5**, 1807-1814.
6. R. Wei, H. Zhang, Z. Hu, T. Qiao, X. He, Q. Guo, X. Tian, Z. Chen and J. Qiu, *Nanotechnology*, 2016, **27**.
7. Z. Chi, H. Chen, Z. Chen, Q. Zhao, H. Chen and Y.-X. Weng, *ACS Nano*, 2018, **12**, 8961-8969.
8. B. T. Diroll, P. Guo, R. P. H. Chang and R. D. Schaller, *ACS Nano*, 2016, **10**, 10099-10105.
9. S. Cha, J. H. Sung, S. Sim, J. Park, H. Heo, M.-H. Jo and H. Choi, *Nat. Commun.*, 2016, **7**, 10768.
10. L. Yang, N. A. Sinitsyn, W. Chen, J. Yuan, J. Zhang, J. Lou and Scott A. Crooker, *Nat. Phys.*, 2015, **11**, 830-834.
11. A. Singh, G. Moody, S. Wu, Y. Wu, N. J. Ghimire, J. Yan, D. G. Mandrus, X. Xu and X. Li, *Phys. Rev. Lett.*, 2014, **112**, 216804.
12. M. Z. Bellus, M. Mahjouri-Samani, S. D. Lane, A. D. Oyedele, X. Li, A. A. Puretzky, D. Geohegan, K. Xiao and H. Zhao, *ACS Nano*, 2018, **12**, 7086-7092.
13. X. Hong, J. Kim, S.-F. Shi, Y. Zhang, C. Jin, Y. Sun, S. Tongay, J. Wu, Y. Zhang and F. Wang, *Nat. Nanotechnol.*, 2014, **9**, 682-686.
14. H. Wang, C. Zhang and F. Rana, *Nano Lett.*, 2015, **15**, 339-345.
15. H. Chen, X. Wen, J. Zhang, T. Wu, Y. Gong, X. Zhang, J. Yuan, C. Yi, J. Lou, P. M. Ajayan, W. Zhuang, G. Zhang and J. Zheng, *Nat. Commun.*, 2016, **7**, 12512.
16. H. Wang, C. Zhang and F. Rana, *Nano Lett.*, 2015, **15**, 8204-8210.
17. C. Poellmann, P. Steinleitner, U. Leierseder, P. Nagler, G. Plechinger, M. Porer, R. Bratschitsch, C. Schüller, T. Korn and R. Huber, *Nat. Mater.*, 2015, **14**, 889-893.
18. M. Wagner, Z. Fei, A. S. McLeod, A. S. Rodin, W. Bao, E. G. Iwinski, Z. Zhao, M. Goldflam, M. Liu, G. Dominguez, M. Thiemens, M. M. Fogler, A. H. Castro Neto, C. N. Lau, S. Amarie, F. Keilmann and D. N. Basov, *Nano Lett.*, 2014, **14**, 894-900.
19. X. Tian, H. Luo, R. Wei, C. Zhu, Q. Guo, D. Yang, F. Wang, J. Li and J. Qiu, *Adv. Mater.*, 2018, **30**, 1801021.
20. C. Zhu, F. Wang, Y. Meng, X. Yuan, F. Xiu, H. Luo, Y. Wang, J. Li, X. Lv, L. He, Y. Xu, J. Liu, C. Zhang, Y. Shi, R. Zhang and S. Zhu, *Nat. Commun.*, 2017, **8**, 14111.
21. F. Wang, T. A. Shifa, X. Zhan, Y. Huang, K. Liu, Z. Cheng, C. Jiang and J. He, *Nanoscale*, 2015, **7**, 19764-19788.
22. Y. Wang, G. Huang, H. Mu, S. Lin, J. Chen, S. Xiao, Q. Bao and J. He, *Appl. Phys. Lett.*, 2015, **107**, 091905.
23. M. Z. Alam, I. De Leon and R. W. Boyd, *Science*, 2016, **352**, 795.
24. M. Z. Alam, S. A. Schulz, J. Upham, I. De Leon and R. W. Boyd, *Nat. Photonics*, 2018, **12**, 79-83.
25. Q. Guo, Y. Cui, Y. Yao, Y. Ye, Y. Yang, X. Liu, S. Zhang, X. Liu, J. Qiu and H. Hosono, *Adv. Mater.*, 2017, **29**, 1700754.
26. N. Kinsey, C. DeVault, J. Kim, M. Ferrera, V. M. Shalaev and A. Boltasseva, *Optica*, 2015, **2**, 616-622.
27. Y. C. Chen, N. R. Raravikar, L. S. Schadler, P. M. Ajayan, Y. P. Zhao, T. M. Lu, G. C. Wang and X. C. Zhang, *Appl. Phys. Lett.*, 2002, **81**, 975-977.
28. H. I. Elim, J. Yang, J.-Y. Lee, J. Mi and W. Ji, *Appl. Phys. Lett.*, 2006, **88**, 083107.